Probing and modifying the empty-state threshold of anatase TiO_2: Experiments and *ab initio* theory

A. Sandell,[1,*] B. Sanyal,[1] L. E. Walle,[2] J. H. Richter,[1] S. Plogmaker,[1] P. G. Karlsson,[1] A. Borg,[2] and P. Uvdal[3]
[1]*Department of Physics and Materials Science, Uppsala University, P.O. Box 530, SE-751 21 Uppsala, Sweden*
[2]*Department of Physics, Norwegian University of Science and Technology, NO-7491 Trondheim, Norway*
[3]*Chemical Physics, Department of Chemistry, Lund University, P.O. Box 124, SE-221 00 Lund, Sweden*
(Received 3 April 2008; revised manuscript received 17 June 2008; published 18 August 2008)

O 1*s* x-ray absorption spectroscopy (XAS) in conjunction with photoelectron spectroscopy has been used to explore the conduction-band edge of single crystalline and nanostructured anatase TiO_2. The experiments are supported by *ab initio* density-functional calculations in which both the initial and core hole final states are considered. The calculations show that the states at the conduction-band edge of anatase are of pure d_{xy} character. This is also the case in the presence of an O 1*s* core hole. In the O 1*s* XAS process pure Ti *d* states cannot be probed and, by appropriate energy referencing, the separation between the Ti *d* derived conduction-band edge and the threshold of the unoccupied Ti *d*–O *p* states can therefore be revealed. The electronic charge needed per Ti to eliminate this offset is discussed in quantitative terms. The theoretical and experimental values are in good agreement, showing that $4 \pm 2\%$ of an electronic charge per Ti ion is sufficient to change the character of the empty states at threshold from pure Ti *d* to Ti *d*–O *p*.

DOI: 10.1103/PhysRevB.78.075113 PACS number(s): 71.20.−b, 73.20.At, 79.60.Bm, 78.70.Dm

I. INTRODUCTION

TiO_2 is a material with a wide range of applications in many different technical areas. It is important within the fields of gas sensors, biocompatible materials, energy storage, photovoltaics, and photocatalysis.[1–4] Most of these applications involve processes where electrons populate empty states in the conduction band. Within the dye sensitized solar cell the first step is light absorption by the dye molecule upon which the excited electron is injected into the TiO_2 conduction band.[5] The key step in photocatalysis is the separation of photoinduced charge carriers.[1,2] Subsequent transfer of holes and electrons between the TiO_2 substrate and the adsorbed molecules govern the surface reactions. Examples of chemical modifications that lead to the population of conduction-band states are Li ion insertion and creation of defects in the form of oxygen vacancies.[3,6–10] Doping of TiO_2 with other transition metals is a modification that has attracted enormous interest recently.[11,12] This largely stems from the prospect of preparing dilute magnetic semiconductors (DMSs) for use in spintronic applications. Whether transition metal doped TiO_2 qualifies as a true DMS is heavily disputed. Still, the system poses many interesting fundamental questions, such as the influence of defects on the magnetic coupling between the dopants.

Anatase TiO_2 is the structural phase that has been the primary choice for applications within the fields of photocatalysis, photovoltaics, and Li ion storage.[1–4,6] Previous theoretical work has revealed ground-state electronic properties unique for the anatase phase of TiO_2.[13] The states at the conduction-band minimum (CBM) are of pure Ti d_{xy} character with the Ti *d*–O *p* mixed states clearly separated from the CBM. This separation is much less pronounced for rutile TiO_2. A considerable optical anisotropy found for anatase was related to the offset between the *d* and *p* thresholds.[13] A transition from the nonbonding p_π states (located at the top of the valence band) to the d_{xy} states is dipole forbidden for the $E \| c$ polarization while it is allowed for the $E \perp c$ polarization. In a theoretical study on the effects of Li insertion in anatase TiO_2 it was furthermore shown that the donated electrons first populate d_{xy} states.[14] At higher *d* populations Ti d_{xz} and d_{yz} states mixed with O *p* states become populated. The orthorhombic distortion of the lattice observed experimentally[15] is not initiated until the Ti d_{yz} states become populated.[14]

Based on the theoretical studies described above it can be concluded that Ti *d*–O *p* mixed states become degenerate with the empty states threshold only above a critical population of the d_{xy} states. This point may define: (i) a change in the transport properties of photoexcited or injected electrons, (ii) a change in the optical properties, and (iii) the onset for geometric changes. Confirming and quantifying these intriguing theoretical findings experimentally is a very important objective. The optimal way to do this is by acquiring high quality experimental data for single-crystal anatase samples. Up to date, the access to anatase single-crystal samples has been very limited. This is in stark contrast to the case of rutile TiO_2 where single crystals of various surface terminations have been readily available for a long time. For this reason rutile TiO_2 has been established as the benchmark metal oxide.

Very recently, studies on the electronic properties of anatase single crystals have started to appear. This allows for fundamental studies of the TiO_2 polymorph primarily used in applications. The results obtained for anatase also serves as the most important complement to the numerous studies of the rutile phase. For example, photoelectron spectroscopy (PES) in a resonant mode has been used to probe the character of the valence band, and important differences between rutile and anatase were highlighted.[16] A significant optical anisotropy has furthermore been found for single-crystal anatase TiO_2.[17] The $E \perp c$ oscillator strength near the absorption edge was found to be one orders of magnitude larger than for $E \| c$. The $E \| c$ and $E \perp c$ absorption edges were assigned to

be direct and indirect optical absorption processes, respectively. This is fully consistent with the theoretical calculations.[13]

In this paper, we use O 1*s* x-ray absorption spectroscopy (XAS) in conjunction with PES to explore the conduction-band edge of single crystalline anatase TiO_2. The experiments are supported by *ab initio* density-functional calculations in which both the initial and core hole final states are considered. We demonstrate that appropriately energy referenced O 1*s* PES and XAS spectra confirm the theoretically predicted separation between the CBM and the Ti 3*d* −O 2*p* mixed states. We furthermore quantify the electronic charge needed per Ti to eliminate this offset, thereby changing the character of the empty states at threshold from pure Ti *d* to Ti *d*−O *p*.

II. EXPERIMENT

The spectra were recorded at the beamlines D1011 and I311 at the Swedish national synchrotron facility MAX II.[18] The end stations at both beamlines comprise a Scienta 200 mm radius hemispherical electron energy analyzer. Binding-energy (BE) calibration was made relative to the Fermi level of a platinum foil mounted on the sample holder. The x-ray absorption spectra were calibrated by the recording of a PES peak excited with first-order and second-order light from the monochromator. The anatase TiO_2 (001) and (101) single crystals (supplied by PI-KEM Ltd., U.K.) were cleaned by cycles of Ar sputtering and subsequent annealing in oxygen to 650 °C. The preparation and characterization of the pristine and Li-modified nanostructured anatase TiO_2 films have been discussed in detail elsewhere.[19,20]

III. CALCULATIONS

Ab initio calculations have been performed by a plane-wave code (VASP) (Ref. 21) within density-functional theory (DFT). A projector augmented wave (PAW) (Ref. 22) basis is used in the local-density approximation (LDA) with Ceperley and Alder exchange-correlation functional parametrized by Perdew and Zunger. We have used a kinetic-energy cutoff of 450 eV for the plane waves included in the basis set. For Brillouin zone integration, *k* points were generated in the Monkhorst Pack scheme. The local density of states (DOS) was calculated by projecting the wave functions onto spherical harmonics. To simulate the final-state effects in the presence of a core hole, we used the $Z+1$ approximation where an impurity with atomic number $Z+1$ is substituted in place of the atom (with atomic number Z), for which spectroscopic measurement is done. For this purpose, we have used the supercell of a $3\times3\times3$ geometry and have placed an F impurity atom in the place of an O atom. The calculations have been done for the anatase phase of TiO_2. The lattice parameters and atomic coordinates were extracted from the experimental results in the literature. The DOS is artificially broadened by a Gaussian function with a full width at half maximum (FWHM) of 0.2 eV.

IV. RESULTS AND DISCUSSION

Figure 1 shows occupied valence electronic states as probed by PES. Clear changes are observed in the valence band depending on the surface studied in line with previous work.[16] An important property is the location of the valence-band edge (VBE). Qualitatively, the results displayed in Fig. 1 suggest that the VBE of the (101) surface is located at a slightly higher BE than that of the (001) surface. DOS calculations show that the VBE of anatase is very sharp.[13] Consequently, the broadening in the experimentally measured VBE is at the present resolution (about 60 meV) dominated by phonons. Fitting of a Gaussian curve therefore yields an estimate of the location of the DOS VBE. These are indicated in Fig. 1. The VBE can also be estimated by use of a linear approach as described in Ref. 23. In the case of semiconductors and metal oxides a common approach is furthermore to assume that the shifts in the VBE position are traced by the BE shifts of the core-level peaks.[24] Since core-level peaks are better defined than the valence band, a more accurate measure of relative shifts of the VBE is provided. In the present case, we have monitored the BE shifts of the Ti 2*p* (4+) and O 1*s* peaks. After applying all three methods described above we estimate that the VBE of the (101) surface is located 0.15 ± 0.05 eV above that of the (001) surface.

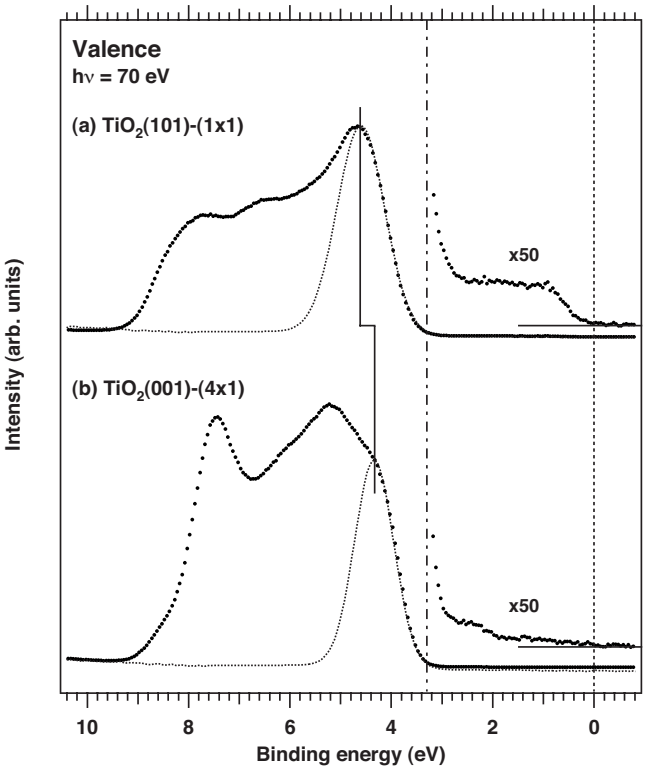

FIG. 1. Valence-band electronic states for (a) TiO_2(101)-(1x1) and (b) TiO_2(001)-(4x1) in the anatase phase. The energy scale is relative to the sample holder Fermi level (dashed line). The Gaussian peaks (dotted) represent the edges of the DOS. The vertical dashed dotted line indicates the experimentally determined optical band gap (Ref. 25) assuming an alignment of the conduction-band edge to the Fermi level.

The binding energy of the VBE relative to the Fermi level is expected to increase upon the population of Ti 3*d* states. It is known that Ti 3*d* states become populated when defects in the form of oxygen vacancies occur, that is, Ti^{3+} states are formed. The (101) surface is more prone to defect formation

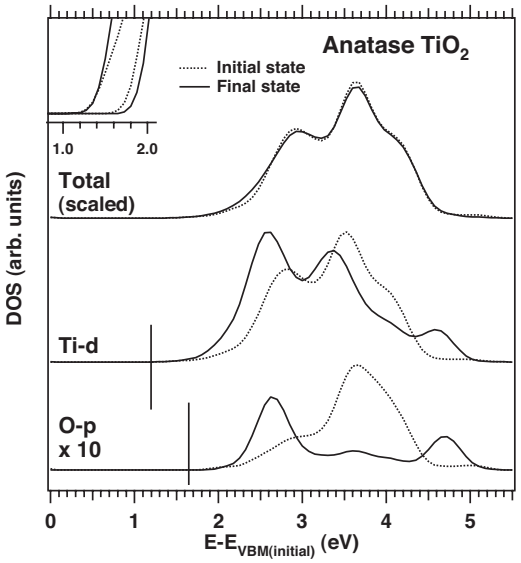

FIG. 2. Total (for the entire unit cell with s, p, and d electrons) and partial (projected on an atom with particular orbital character) density of states for anatase TiO_2 obtained by *ab initio* calculations. The energy scale is relative to the valence-band maximum of the initial state. Dashed lines: DOS curves for the initial state. Solid lines: DOS curves for the final state with an O 1s core hole present. The total density of states is scaled in order to facilitate a comparison. As indicated, the O-p DOS is comparable to the Ti-d DOS if divided by a factor of ten. The Ti-d and O-2p onsets of the final states are marked with vertical solid lines. The inset shows a magnified view of the different Ti-d and O-2p onsets for anatase.

than the (001) surface as pointed out previously.[16] A weak Ti 3d related feature at 1 eV BE is indeed observed for the (101) surface, while no Ti 3d state can be discerned for the (001) surface. (It can be noted that both spectra exhibit a much lower defect density than those previously reported.) By normalizing to a sputtered and annealed surface where reduced states are clearly visible in the Ti 2p spectrum, it was possible to estimate the Ti^{3+} density to $1.0 \pm 0.5\%$ per Ti ion for the (101) surface. (The difficulty in defining the background is the major cause of a rather large error.) The presence of a Ti 3d feature is consistent with the positive binding-energy shift of the VBE for the (101) surface when compared with the (001) surface.

Most important for the analysis is to determine the location of the CBM. There are two observations that suggest that the CBM is well aligned to the Fermi-level reference. First, the expanded spectra show populated band-gap states reaching up to a point that coincides with the Fermi level (Fig. 1). Second, the band gap of anatase TiO_2 is reported to be
3.3 eV.[25] When taking this value relative to the Fermi level (dashed dotted line in Fig. 1), the position agrees very well with the low BE onset of the valence band. Thus, the energy difference between the VBE and the Fermi level agrees very well with the band-gap energy given by optical absorption.

Figure 2 shows the calculated unoccupied DOS for anatase TiO_2. The curves for the initial and final states are included, aligned against the VBE of the initial state. The partial DOS curves show clearly that the unoccupied states in this energy region are predominantly of Ti 3d character with a small admixture of O 2p. The states closest to the CBM are however of pure Ti 3d character. The ground-state calculations presented are in very good agreement with previous work.[13] The final-state DOS reveal significant effects upon the formation of an O 1s core hole. The weight of the Ti 3d DOS and O 2p DOS moves closer to threshold and the integrated O 2p DOS decreases. An increased population of the O 2p states is expected given that the final state can be envisaged as a fluorine ion according to the $Z+1$ approximation. Most important, however, is that the offset between the Ti 3d DOS and the O 2p onsets is retained. The offset between the Ti 3d DOS and the O 2p onsets amounts to 0.45 eV. The spatial distribution of the states at the CBM confirms that these are made up of nonbonding Ti $3d_{xy}$ states (not shown).

The fact that the offset is retained in the presence of an O 1s hole strongly suggests that it is present also upon the formation of a hole in the valence band. This lends strong support for the interpretation that the large optical dichroism is correlated with the existence of nonbonding d_{xy} states at the bottom of the conduction band.[13]

That the offset is present upon the creation of an O 1s hole justifies furthermore the use of O 1s XAS to probe the properties of the empty states threshold. The symmetry condition and the strong core hole localization leads to population of states of predominantly O p character in the O 1s XAS process.[26] Hence pure Ti d states cannot be probed and a central issue is therefore to determine the position of the CBM in the O 1s XAS spectrum. This can be accomplished by a comparison with the O 1s PES spectrum. Figures 3(a) and 3(b) show O 1s XAS and PES spectra for anatase (001) and (101), respectively. The XAS and PES spectra are placed on a common energy scale. The energy values of the PES spectra are relative to the Fermi level, whereas the energy values of the XAS spectra correspond to the absolute photon energy. The spectra are normalized as to have the same peak height. The final-state calculations show an unoccupied O p DOS that is sharp at threshold. Together with additional dynamical effects[27] this results in nearly identical shapes of the XAS edge and the low BE side of the O 1s PES line.[28] That is, the shape of the XAS threshold is predominantly influenced by phonon excitations, similar to the VBE. Consequently, the DOS threshold is given by the position of the leading XAS peak.[27,28] With this in mind it stands clear from Figs. 3(a) and 3(b) that the DOS threshold as probed by O 1s XAS is well separated from the Fermi level for both surfaces. This separation is associated with the aforementioned offset between the pure d states at the CBM and the p-d states reachable in the O 1s XAS process. The offset is 0.6 ± 0.1eV for the (001) surface and 0.4 ± 0.1eV for the (101) surface. The difference in the offset furthermore matches the difference in the VBE location very well, which suggests a rigid shift of the electronic levels.

The nanostructured anatase TiO_2 film provides very important information on the O p-CBM offset since the Ti d population can be increased in a controlled fashion by Li insertion. Insertion of lithium leads to electron donation from the Li 2s orbital to Ti 3d states.[9,14,29] As a result, the gap between the CBM and the O 2p empty DOS is expected to

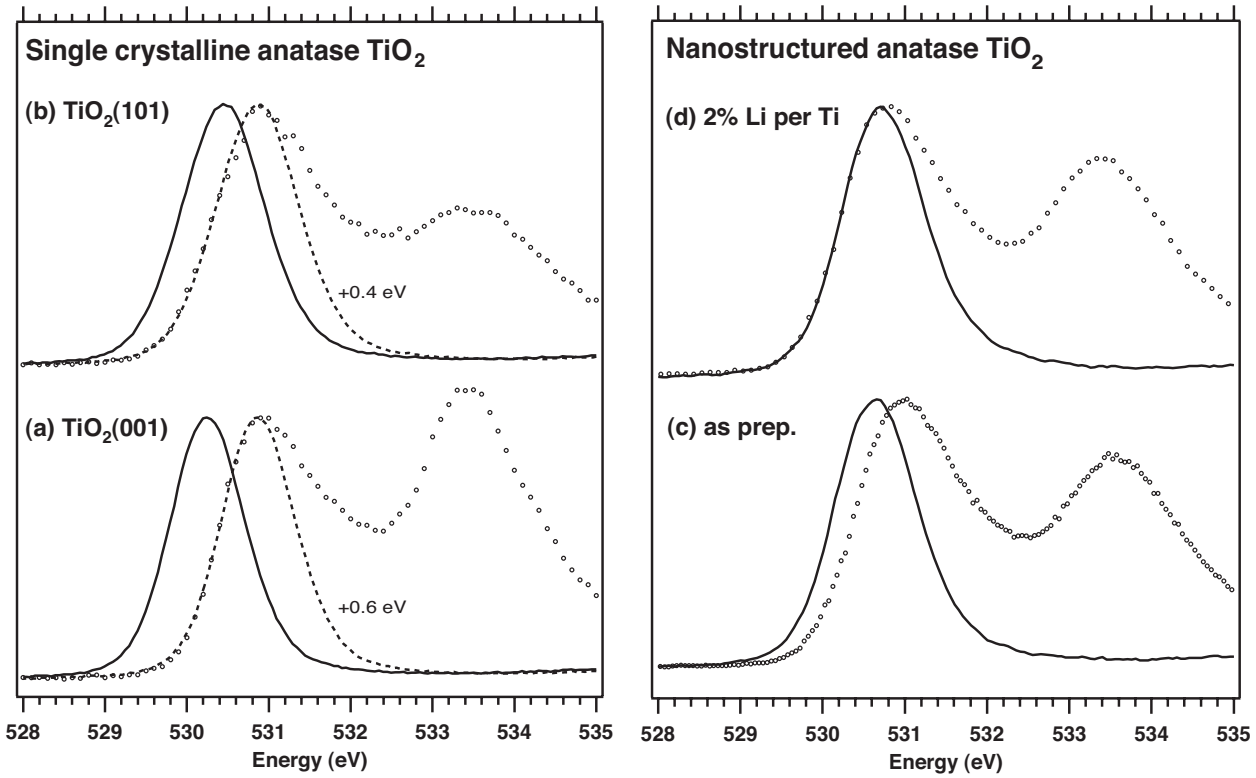

FIG. 3. O 1*s* XAS and PES spectra for anatase (a) TiO_2(001)-(4x1) and (b) TiO_2(101)-(1x1) on a common energy scale. The energy values of the PES spectra are relative to the Fermi level, whereas the energy values of the XAS spectra correspond to the absolute photon energy. The spectra are normalized as to have the same peak height. A clear separation between the XAS and PES peaks are observed for both surfaces with a smaller separation noted for the (101) surface. (c) The same comparison for an as-prepared nanostructured anatase film also reveals an XAS–PES separation. As shown in (d), this offset can be eliminated by the insertion of small amounts of lithium.

decrease. At sufficient Li concentration the O 2*p* DOS threshold will become degenerate with the empty states threshold.

The valence spectra before and after insertion of Li are shown in Fig. 4. The as-prepared film exhibits a small Ti 3*d* peak at 1 eV BE due to defects. Upon insertion of 2% Li per Ti ion the intensity of the Ti 3*d* state increases significantly and the valence band shifts toward higher BE. The O 1*s* PES-XAS relationship for the as-prepared nanostructured anatase film is qualitatively similar to the single-crystal surfaces. Figure 3(c) shows that the binding energy of the O 1*s* PES line relative to the Fermi level is about 0.3 eV lower than the photon energy of the XAS peak. Figure 3(d) shows that the PES-XAS offset for the as-prepared anatase film is eliminated by the addition of only 2% Li per Ti ion. That is, the Fermi-level referenced binding energy of the O 1*s* peak has become identical to the photon energy of the leading O 1*s* XAS peak. Since no further shift of the O 1*s* BE is found at higher Li concentrations,[29] the matching of the O 1*s* PES peak to the XAS peak remains. The conclusion that the population of *d* states eventually eliminates the O 1*s* PES-XAS separation is supported by the results for the (101) surface. Extended sputtering leads to an additional shift of $+0.35 \pm 0.05$eV, in very good agreement with the 0.4 eV offset found for the pristine surface.

The results are summarized in Fig. 5. The CBM-O *p* offset, as determined from the O 1*s* PES and XAS results—is plotted as a function of the additional Ti *d* population for the different experimental situations. (The word "additional" is used to take the small *d* character of the valence band into consideration.) The offset at zero additional Ti *d* population is set to 0.6 ± 0.1 eV, which is the value for the (001) sur-

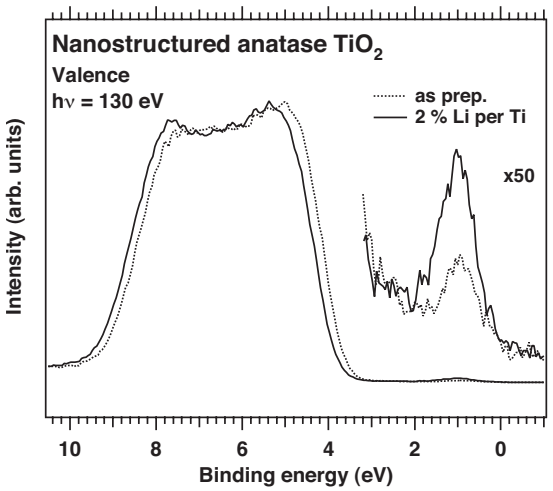

FIG. 4. Valence-band electronic states for an *in situ* prepared film of anatase TiO_2 nanoparticles before (dotted line) and after (solid line) insertion of 2% Li per Ti ion. The binding-energy scale is referenced to the sample holder Fermi level. The addition induces an increase in the intensity of the Ti 3*d* related band-gap state and a positive binding-energy shift of the valence band.

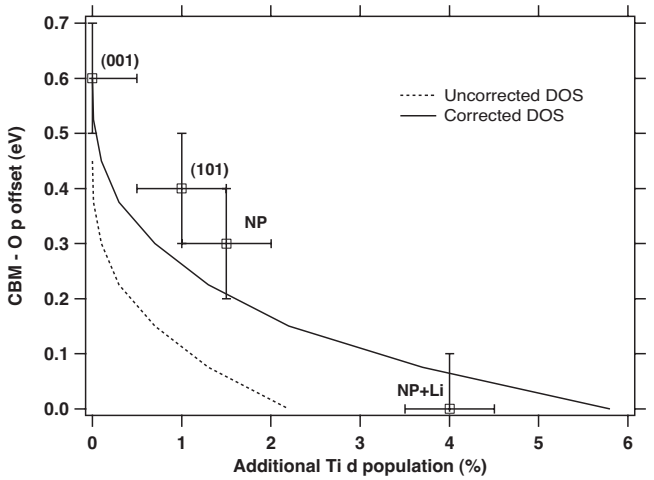

FIG. 5. Squares: The experimental offset between the conduction-band minimum and the threshold of the unoccupied O *p* states as a function of the additional Ti *d* population estimated from the intensity of the band-gap state. The dashed and solid lines show the offset as a function of the additional Ti *d* population for the uncorrected and corrected (shifted) calculated DOSs, respectively.

face. A progressive decrease is observed as qualitatively expected, with an elimination of the CBM—O *p* offset at about 4% *d* population per Ti.

In quantitative terms, it is the shape of the *d* band that determines the decrease in the offset as a function of the additional *d* population. This motivates a comparison with the theoretical results. The dashed line is derived from the calculated final-state DOS, whereas the solid line is for the shifted O-*p* edge toward higher energy. It is well known that DFT produces much smaller band gap of semiconductors and insulators. Often a scissor operator is employed to correct the band gap by shifting the band edges in order to fit with the experimental band gap. Here, a similar concept is used to shift the O-*p* edge by 0.15 eV to match the experimentally observed offset of 0.6 eV for zero additional *d* population. We find that this operation results in a significantly improved agreement. However, we emphasize that this shift should be regarded only as a way to fit the theory with the experimental observations.

The results have a clear relevance to the many applications of TiO_2 where the properties near the CBM are important, such as photovoltaic cells and photocatalysis. The results are also of importance for the understanding of TiO_2 modified by the addition of small amounts of other elements. In particular, this work can be an important input to the intense debate concerning room-temperature ferromagnetism (RTFM) in anatase TiO_2 doped with magnetic elements.[8] In the case of Co-doped TiO_2 oxygen vacancies (O_{vac}) are needed in order to charge compensate for the replacement of Ti^{4+} with Co^{2+}. The O_{vac} electrons are believed to reside close to the Co^{2+} sites. However, it has become clear that additional oxygen vacancies are required to provide charge carriers for achieving RTFM in an *n*-type DMS.[8] Such additional oxygen vacancies result in the population of TiO_2 CB states. As the hybridization between the transition metal *d* states and the O *p* states may become crucial for ferromagnetism, the character of the electronic states near CBM is important to understand. It is finally intriguing to note that the typical Co concentrations needed for RTFM (1%–7% per Ti ion) matches well the critical concentration for the change in the character of the populated band-gap states of TiO_2. Whether this is pure coincidence or not remains to be elucidated.

With respect to the general applicability of the approach involving O 1*s* core-level spectroscopy in conjunction with calculations, we can compare it with our previous work on ZrO_2.[28,30] The results for TiO_2 and ZrO_2 have in common that the leading O 1*s* XAS peak, when related in energy to the valence band, represents the onset for the O *p* empty states. The core hole appears to modify the intensity distribution of the empty DOS but not the energy position of the threshold. We therefore propose that O 1*s* XAS combined with O 1*s* PES is a general method to locate the O *p* empty states threshold for transition metal oxides. In the case of ZrO_2 the O *p* empty states threshold is degenerate with the CBM. O 1*s* core-level spectroscopy can therefore be used to monitor the position of the CBM.[28,30] However, the threshold for the empty O *p* states is not always degenerate with the CBM. Anatase TiO_2 is one example where this occurs. The kind of information derived from this particular experimental approach can therefore change depending on the electronic properties of the material under study. In order to define the issue to address supporting information from calculations or other experimental techniques is essential.

V. CONCLUSIONS

In summary, PES, XAS, and *ab initio* density-functional calculations have been used to study the properties of the electronic states located at or near the CBM of anatase titanium dioxide. In agreement with previous work we find that the states at the CBM are of pure Ti d_{xy} character. States with *p*-*d* character are offset from the CBM and can only be populated after a critical d_{xy} population has been reached. This point can be reached by creation of defects in the form of oxygen vacancies or by Li insertion. The theoretical and experimental estimates of the critical population are in good agreement, giving a value of about $4 \pm 2\%$ of an electronic charge per Ti ion.

ACKNOWLEDGMENTS

We thank the staff at MAX-laboratory for their excellent assistance. The authors are grateful to the Swedish Science Council (VR), the Göran Gustafsson Foundation, the Knut and Alice Wallenberg (KAW) Foundation, and the Crafoord Foundation for the financial support. B.S. acknowledges the Swedish National Infrastructure for Computing (SNIC) for the allocation of computational time.

*Corresponding author. Fax: +46 18 4713524.
anders.sandell@fysik.uu.se.

[1] O. Carp, C. L. Huisman, and A. Reller, Prog. Solid State Chem. **32**, 33 (2004).
[2] A. L. Linsebigler, G. Lu, and J. T. Yates, Chem. Rev. (Washington, D.C.) **95**, 735 (1995).
[3] U. Diebold, Surf. Sci. Rep. **48**, 53 (2003).
[4] M. Ni, M. K. H. Leung, D. Y. C. Leung, and K. Sumathy, Renewable Sustainable Energy Rev. **11**, 401 (2007).
[5] B. O'Regan and M. Grätzel, Nature (London) **353**, 737 (1991).
[6] S. Y. Huang, L. Kavan, I. Exnar, and M. Grätzel, J. Electrochem. Soc. **142**, L142 (1995).
[7] A. Henningsson, H. Rensmo, A. Sandell, H. Siegbahn, S. Södergren, H. Lindström, and A. Hagfeldt, J. Chem. Phys. **118**, 5607 (2003).
[8] M. Wagemaker, D. Lützenkirchen-Hecht, A. A. van Well, and R. Frahm, J. Phys. Chem. B **108**, 12456 (2004).
[9] J. H. Richter, A. Henningsson, B. Sanyal, P. G. Karlsson, M. P. Andersson, P. Uvdal, H. Siegbahn, O. Eriksson, and A. Sandell, Phys. Rev. B **71**, 235419 (2005).
[10] C. Di Valentin, G. Pacchioni, and A. Selloni, Phys. Rev. Lett. **97**, 166803 (2006).
[11] S. A. Chambers, Surf. Sci. Rep. **61**, 345 (2006).
[12] J. Osorio-Guillén, S. Lany, and A. Zunger, Phys. Rev. Lett. **100**, 036601 (2008).
[13] R. Asahi, Y. Taga, W. Mannstadt, and A. J. Freeman, Phys. Rev. B **61**, 7459 (2000).
[14] M. V. Koudriachova, S. W. de Leeuw, and N. M. Harrison, Phys. Rev. B **69**, 054106 (2004).
[15] R. J. Cava, D. W. Murphy, S. Zahurak, A. Santoro, and R. S. Roth, J. Solid State Chem. **53**, 64 (1984).
[16] A. G. Thomas, W. R. Flavell, A. K. Mallick, A. R. Kumarasinghe, D. Tsoutsou, N. Khan, C. Chatwin, S. Rayner, G. C. Smith, R. L. Stockbauer, S. Warren, T. K. Johal, S. Patel, D. Holland, A. Taleb, and F. Wiame, Phys. Rev. B **75**, 035105 (2007).
[17] N. Hosaka, T. Sekiya, C. Aatoko, and S. Kurita, J. Phys. Soc. Jpn. **66**, 877 (1997).
[18] R. Nyholm, J. N. Andersen, U. Johansson, B. N. Jensen, and I. Lindau, Nucl. Instrum. Methods Phys. Res. A **467-468**, 520 (2001); J. N. Andersen, O. Björneholm, A. Sandell, R. Nyholm, J. Forsell, L. Thånell, A. Nilsson, and N. Mårtensson, Synchrotron Radiat. News **4**, 15 (1991).
[19] A. Sandell, M. P. Andersson, Y. Alfredsson, M. K.-J. Johansson, J. Schnadt, H. Rensmo, H. Siegbahn, and P. Uvdal, J. Appl. Phys. **92**, 3381 (2002).
[20] A. Henningsson, M. P. Andersson, P. Uvdal, H. Siegbahn, and A. Sandell, Chem. Phys. Lett. **360**, 85 (2002).
[21] G. Kresse and J. Hafner, Phys. Rev. B **47**, 558 (1993); G. Kresse and J. Furthmüller, *ibid.* **54**, 11169 (1996).
[22] P. E. Blöchl, Phys. Rev. B **50**, 17953 (1994).
[23] S. A. Chambers, Y. Liang, Z. Yu, R. Droopad, J. Ramandi, and K. Eisenbeiser, Appl. Phys. Lett. **77**, 1662 (2000).
[24] R. Puthenkovilakam and J. P. Chang, Appl. Phys. Lett. **84**, 1353 (2004).
[25] G. K. Boschloo, A. Goossens, and J. Schoonman, J. Electrochem. Soc. **144**, 1311 (1997).
[26] J. Stöhr, *NEXAFS Spectroscopy*, Springer Series in Surface Science Vol. 25 (Springer-Verlag, Heidelberg, 1992).
[27] E. O. F. Zdansky, A. Nilsson, H. Tillborg, O. Björneholm, N. Mårtensson, J. N. Andersen, and R. Nyholm, Phys. Rev. B **48**, 2632 (1993).
[28] J. H. Richter, P. G. Karlsson, B. Sanyal, J. Blomquist, P. Uvdal, and A. Sandell, J. Appl. Phys. **101**, 104120 (2007).
[29] J. H. Richter, A. Henningsson, P. G. Karlsson, M. P. Andersson, P. Uvdal, H. Siegbahn, and A. Sandell, Phys. Rev. B **71**, 235418 (2005).
[30] A. Sandell, P. G. Karlsson, J. H. Richter, J. Blomquist, P. Uvdal, and T. M. Grehk, Appl. Phys. Lett. **88**, 132905 (2006).